Materials Science-Poland, 38(1), 2020, pp. 165-173
http://www.materialsscience.pwr.wroc.pl/
DOI: 10.2478/msp-2020-0020

sciendo

Hafnium dioxide effect on the electrical properties of M/n-GaN structure

SADOUN ALI[1,*], MANSOURI SEDIK[1], CHELLALI MOHAMMED[1], LAKHDAR NACEREDDINE[2], HIMA ABDELKADER[2], BENAMARA ZINEB[1]

[1]Laboratoire de Micro-Electronique Appliquée, Université Djillali Liables de Sidi Bel Abbes, BP 89, 22000 Sidi Bel Abbes, Algeria

[2]University of El Oued, Fac. Technology, 39000 El Oued, Algeria

In the present paper, using of SILVACO-TCAD numerical simulator for studying the enhancement in Pt/n-GaN Schottky diode current–voltage (I-V) characteristics by introduction of a layer of hafnium dioxide (HfO_2) (with a thickness e = 5 nm) between the Pt contact and semiconductor interface of GaN is reported. The simulation of I-V characteristics of Pt/n-GaN was done at a temperature of 300 K. However, the simulation of Pt/HfO_2/n-GaN structure was performed in a temperature range of 270 – 390 K at steps of 30 K. The electrical parameters: barrier height (Φ_b), ideality factor and series resistance have been calculated using different methods: conventional I-V, Norde, Cheung, Chattopadhyay and Mikhelashvili. Statistical analysis showed that the metal-insulator-semiconductor (Pt/HfO_2/n-GaN) structure has a barrier height of 0.79 eV which is higher compared with the (Pt/n-GaN) structure (0.56 eV). The parameters of modified Richardson $((\ln\left(\frac{I_0}{T^2}\right) - \left(\frac{q^2\sigma_{s0}^2}{2kT^2}\right) = \ln(AA^*) - \frac{q\varnothing_{B0}}{kT})$ equation versus $(\frac{1}{kT})$ have been extracted using the mentioned methods. The following values: $A^*_{Simul} = 22.65$ A/cm$^2\cdot$K^2, 14.29 A/cm$^2\cdot$K^2, 25.53 A/cm$^2\cdot$K^2 and 21.75 A/cm$^2\cdot$K^2 were found. The Chattopadhyay method occurred the best method for estimation the theoretical values of Richardson constant.

Keywords: *Schottky diode; Pt/n-GaN; Pt/HfO_2/n-GaN; (I-V), Norde, Cheung, Mikhelashvili and Chattopadhyay methods; modified Richardson equation.*

1. Introduction

The III-V semiconductors family is widely used in manufacturing of electronic components such as Schottky diodes (MS), metal-insulator-semiconductor (MIS) and metal-oxide-semiconductor (MOS) transistors, etc. [1–4]. GaN binary compound is a direct band gap semiconductor with $E_g = 3.22$ eV and lattice parameter a = 4.52Å at 300 K [5] that belongs to III-V family. This binary compound is a promising material for light-emitting diodes (LEDs), photodetectors (MSMs), laser diodes (LDs), solar cells and microwave field effect transistors [6–10]. GaN high frequency characteristics make it suitable for high frequency and high power applications [11].

The application of GaN in metal-insulator-semiconductor devices studies attracted researchers attention, especially in electrical characterization of MIS nitride interfaces, in which the most important insulator is hafnium dioxide (HfO_2). Hafnium dioxide (HfO_2) – a binary compound has proven to be one of the most high-k dielectrics because of its excellent dielectric properties, high melting point [12, 13], wide band gap (calculated $E_g = 5.10$ eV and experimental $E_g = 5.12$ eV) and lattice parameter a = 4.98Å (local density approximation LDA) at 300 K [14, 15]. This binary compound is a promising material for MOSFET [16] and MIS. In this context, hafnium dioxide (HfO_2) may play a crucial role as an interfacial layer in GaN-based Schottky diodes and it is important to understand the electrical behavior of Pt/HfO_2/n-GaN-based structures.

There have been many experimental and theoretical studies on the fabrication of Schottky diodes (metal- GaN) devices. Among these studies, Varra Niteesh Reddy et al. [17] performed an

*E-mail: 3ali39@gmail.com

© 2020. This is an open access article distributed under the Creative Commons Attribution-NonCommercial-NoDerivatives 4.0 License. (http://creativecommons.org/licenses/by-nc-nd/4.0/)

analysis of electronic parameters and frequency-dependent properties of Au/NiO/n-GaN Schottky diodes at various frequencies in the range of 1 kHz – 1 MHz. V. Rajagopal Reddy et al. [18] reported electrical properties and current transport mechanism in $Au/BaTiO_3$/n-GaN structures that have been investigated by current-voltage (I-V) and capacitance-voltage (C-V) measurements at a temperature of 300 K. B. Prasanna Lakshmi et al. [19] studied the effect of temperature on the electrical properties of Au/Ta_2O_5/n-GaN structures at various temperatures in the range of 400 – 600 K. C. Venkata Prasad et al. [20] investigated electrical and carrier transport properties of an Au/Y_2O_3/n-GaN diode with rare-earth oxide interlayer. M. Siva Pratap Reddy et al. [21] investigated temperature effect on electrical properties and carrier transport mechanism in the $Ni/Au/Al_2O_3$/GaN diode in the range of 150 – 400 K.

In this paper, numerical simulations (Sim.) of (Pd/n-GaN) Schottky diode containing a layer of hafnium dioxide have been presented. The effect of hafnium dioxide layer on electrical properties of (Pd/n-GaN) structure at a wide temperature range (270 K – 390 K) has been discussed in order to enhance the electrical performance of Schottky diode-based structures. Therefore, our work is extended to study the evolution of barrier height (Φ_{b0}), ideality factor (n) and series resistance (R_s) using (I-V), Norde, Cheung and Cheung, Chattopadhyay and Mikhelashvili methods. The obtained results are in agreement with experimental and theoretical ones. Our numerical simulations have been performed using SILVACO-TCAD software.

2. Modeling

In order to elucidate the observed effect of temperature on the (Pt/HfO_2/GaN) structure performance, modeling and simulation have been carried out using the ATLAS module of the SILVACO-TCAD software based on work of Arjun Shetty et al. [22]. The parameters used in the simulation are listed in Table 1 with corresponding references for each value. The Schottky diode was assumed to be operating under standard conditions, in temperature range (270 K –390 K).

3. Result and discussion

3.1. Current-voltage (I-V) method

The effect of diode resistance can be modeled by a series combination of a diode and a resistor (Rs) through which the current flows. In addition, in the case of an ideal diode, ideality factor (n) equals 1, while for a real diode the n value is higher than 1 (n >1). In the case of Schottky diode, assuming that the current is due to a thermionic emission (TE), the relation between the applied forward bias and the current can be given by equation 1 [18, 27, 28].

$$I = I_0 \exp\left(\frac{-qV}{kT}\right)\left[1-\exp\left(\frac{q(V-IR)}{nkT}\right)\right] \quad (1)$$

where I_0, n, k and T are the reverse saturation current, the ideality factor, the Boltzmann constant, the absolute temperature in Kelvin, respectively. We could find the value of (I_0) by plotting lnI versus V and extrapolating the curve to V = 0 V. Then, by replacing the calculated (I_0) value in the equation 2

$$I_0 = AT^2A^*\exp\left(\frac{q\Phi_{b0}}{kT}\right) \quad (2)$$

where A is the rectifier contact area, A^* is the Richardson constant (A^* = 26.4 A/cm^2·K^2 for n-GaN [29]) and Φ_b is the Schottky barrier height. The value of Φ_b can and calculated by equation 3

$$\Phi_{b0} = \frac{kT}{q}\ln\left(\frac{AA^*T^2}{I_0}\right) \quad (3)$$

Fig. 1 shows the current-voltage (I-V) characteristics of Pt/GaN Schottky diode, at atemperature of 300 K, and Pt/HfO_2/GaN diode, at some selected temperatures (270, 300, 330, 360 and 390 K) in a semi-logarithm scale. The obtained simulation results for the saturation current (I_0), barrier height (Φ_b) and ideality factor (n) are shown in Table 2.

The value of experimental ideality factor (n) matched with the simulated value, and the experimental barrier height (Φ_b) value is a bit smaller than the simulated value in temperature range of 270 – 390 K. According to the obtained results, we observed that increasing of temperature is accompanied with decreasing of the ideality factor and the

Table 1. Parameters of HfO_2 used in the simulation at T = 300 K.

Parameter	Symbol	Value	Ref
Thickness [nm]	$e_{(HfO2)}$	5	[22]
Band gap [eV]	$Eg_{(HfO2)}$	5.7	[23]
Contact work function [eV]	Φ_n	5.65	[24]
Electron affinity [eV]	χ	1.75	[25]
Dielectric constant	ϵ	25	[26]

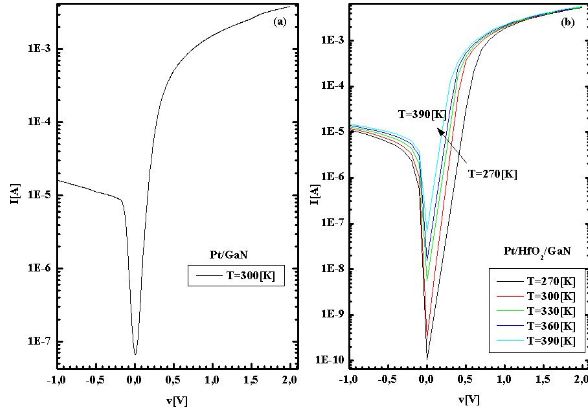

Fig. 1. I-V characteristics of Pt /GaN (a) at T = 300 K and (b) Pt/HfO_2/GaN for T = 270, 300, 330, 360 and 390 K.

barrier height increase. Consequently, due to the low energy, the charge carriers are not able to cross the large barrier height at these temperatures. However, current transport is provided by lower parts of barrier height [30, 31].

3.2. Cheung method

The ideality factor (n), the Schottky barrier height (Φ_b) and the series resistance (Rs) have been calculated by a second method called Cheung and Cheung [32]. In this method, ideality factor (n) and the series resistance (Rs) can be obtained using the derivative ($\frac{\partial V}{\partial(\ln(I))}$) that is determined in equation 4 [32]:

$$G = \frac{\partial V}{\partial(ln(I))} = \frac{nkT}{q} + I\,Rs \quad (4)$$

Also, Schottky barrier height (Φ_b), can be defined by Cheung's (H(I)) relation presented by equation 5 [32]:

$$H(I) = V - \left(\frac{nkT}{q}\right) ln\left(\frac{I}{AA^*T^2}\right) = n\,\Phi_{bn} + IR_S \quad (5)$$

Fig. 2a – c shows the obtained curves of $\left(\frac{dV}{d(\ln(I))}\right)$ and H(I) as a function of I for Pt/GaN structure and for Pt/HfO_2/GaN structure, at different temperatures (270, 300, 330, 360 and 390 K). The values of the ideality factor (n), the Schottky barrier height (Φ_b) and the series resistance (Rs) were determined from these curves and presented in Table 2.

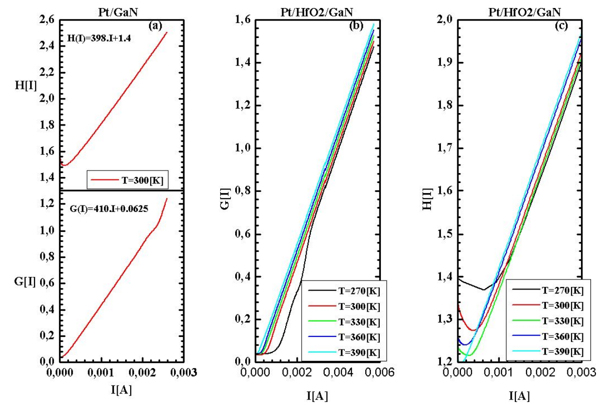

Fig. 2. (a) $\frac{dV}{d(\ln(I))}$ and H (I) as a function of I for Pt/GaN at T = 300 K, (b) $\frac{dV}{d(\ln(I))}$ as a function of I for Pt/HfO_2/GaN, (c) H (I) as a function of I for Pt/HfO_2/GaN at T = 270, 300, 330, 360 and 390 K.

3.3. Norde method

Alternatively, the Norde approximation [33] can be used. This approximation is based on a modified forward current-voltage (I-V) plot that can be

Table 2. Values of saturation current, barrier height, ideality factor and series resistance for Pt/GaN and $Pt/HfO_2/GaN$ structures in the temperature range 270 K – 390 K.

	Pt/GaN		Pt/HfO_2 /GaN									
T[K]	300		270		300		330		360		390	
	Sim.	Exp. [22]	Sim.	Exp. [22]	Sim.	Exp. [22]	Sim.	Exp. [22]	Sim.	Exp. [22]	Sim.	Exp.
I- V method												
$I_0 \cdot 10^{-8}$ [A]	6.5	–	102	–	416	–	56.0	–	1.52	–	6.82	–
Φ_b [eV]	0.56	0.54	0.74	0.53	0.79	0.63	0.80	0.70	0.85	0.77	0.87	–
n	2.01	2.10	1.82	1.80	1.33	1.30	1.28	1.42	1.23	1.30	1.20	–
R_S [Ω]	257	–	285	–	277	–	272	–	267	–	263	–
Cheung' s method G(I)												
n	2.50	–	1.90	–	1.75	–	1.58	–	1.50	–	1.42	–
R_S [Ω]	410	–	266	–	263	–	262	–	260	–	248	–
Cheung' s method H(I)												
Φ_b [eV]	0.56	–	0.61	–	0.68	–	0.75	–	0.80	–	0.83	–
R_S [Ω]	398	–	272	–	267	–	262	–	260	–	258	–
Norde's method												**–**
Φ_b [eV]		–	0.68	–	0.76	–	0.77	–	0.79	–	0.81	–
Chattopadhyay's method												**–**
n	1.98	–	1.81	–	1.72	–	1.42	–	1.35	–	1.25	–
Φ_b [eV]	0.60	–	0.66	–	0.70	–	0.76	–	0.81	–	0.83	–
Mikhelashvili's method												
Φ_b [eV]	0.59	–	0.64	–	0.69	–	0.74	–	0.75	–	0.77	–
n	2.11	–	3.10	–	2.12	–	2.00	–	1.95	–	1.89	–
R_S [Ω]	450	–	269	–	260	–	207	–	160	–	158	–

used to calculate the parameters: series resistance (Rs) and barrier height (Φ_b) of both structures. The Norde approximation is defined by equation 6 [33]:

$$F(v) = \frac{v}{\gamma} - \frac{kT}{q} \ln\left(\frac{I(v)}{AA^{*}T^{2}}\right) \tag{6}$$

where γ is an integer (dimensionless) greater than n (n = 2.01) and the I(V) represents the current which is acquired from the (I-V) curve. In this approximation, Φ_b and Rs values can be determined using equation 7 [33, 34]:

$$\Phi_b = F(v_0) + \left[\frac{v_0}{\gamma} - \frac{kT}{q}\right] \tag{7}$$

where n value is obtained from the ln I-V curve, $F(v_0)$ is the minimum point of F(v) plot, v is the corresponding voltage.

Fig. 3a and Fig. 3b show the evolution of Norde's function F(v) of V obtained from forward bias (I-V) characteristics of the (Pt/GaN or $Pt/HfO_2/GaN$) structures. The results of barrier height (Φ_b) are shown in Table 2.

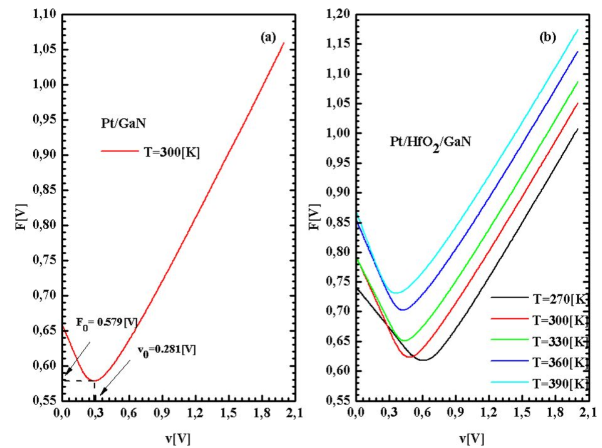

Fig. 3. F (V) as a function of V obtained from forward bias current-voltage characteristics of (a) Pt /GaN at T = 300 K and (b) Pt $/HfO_2/Ga$ for T = 270, 300, 330, 360 and 390 K.

From Fig. 3a, we can determine the values of F(v) and (v) that are equal to 0.579 and 0.281 V, respectively, at temperature of 300 K.

3.4. Chattopadhyay model

This approximation can be used to determine the barrier height (Φ_b) and the ideality factor (n) values from Ψs(V) behavior shown in Fig. 4. The barrier height (Φ_b), can be calculated from the equation 8 [35]:

$$\varphi_b = \Psi_s(J_C, V_C) + C_2 V_C + V_n - \frac{KT}{q} \tag{8}$$

where V_n is the potential difference between the Fermi level (E_F) and the bottom of the conduction band (E_c), which can be written as shown in equation 9:

$$V_n = \frac{kT}{q} \ln\left(\frac{N_c}{N_d}\right) \tag{9}$$

where, N_c and N_d present the effective conduction band density of states and the carrier concentration, respectively. The calculated V_n values are equal to 0.073, 0.081, 0.087, 0.097 and 0.104 eV corresponding with 270, 300, 330, 360 and 390 K, respectively.

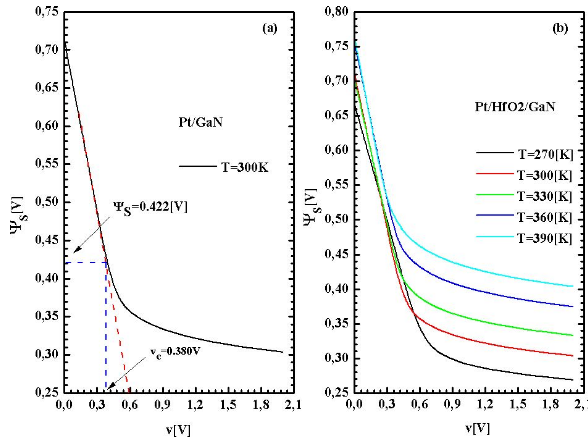

Fig. 4. Surface potential-forward voltage curves of (a) the Pt/GaN at T = 300 K and (b) the $Pt/HfO_2/GaN$ for T = 270, 300, 330, 360 and 390 K.

The value of surface potential Ψ_s is given in equation 10 [35, 36]:

$$\Psi_s = \frac{kT}{q} \ln\left(\frac{AA^* T^2}{I}\right) - Vn \tag{10}$$

From Fig. 4, we have determined the values of Ψ_s and V_C (critical voltage) that are equal to 0.36, 0.39, 0.42, 0.47, 0.52 eV and 0.54, 0.44, 0.39, 0.38, 0.29 eV, respectively, for corresponding temperatures of 270, 300, 330, 360 and 390 K. The inverse of the ideality factor (C_2) can be determined by equation 11:

$$C_2 = \frac{1}{n} = \left(\frac{d\Psi_s}{dV}\right)_{Jc,Vc} \tag{11}$$

With the aid of equations 8 and 11, the values of ideality factor (n) and barrier height (Φ_b) were obtained and collected in Table 2.

3.5. Mikhelashvili method

Another technique for determination of the barrier height (Φ_b), the ideality factor (n) and the series resistance (Rs) is called Mikhelashvili's method [35]. This method is based on the equation 12:

$$\theta(v) = \frac{d(\ln(I))}{d(\ln(v))} \tag{12}$$

The ideality factor (n) and the barrier height (Φ_b) are obtained from equations 13 and 14:

$$n = \frac{q v_m (\theta_m - 1)}{kT \theta_m^2} \tag{13}$$

$$\Phi_b = \frac{kT}{q}\left[\theta_m + 1 - \ln\left(\frac{I_m}{AA^* T^2}\right)\right] \tag{14}$$

where: θ_m and V_m are the coordinates of maximum point in θ (V) versus V plot shown in Fig. 5. We determined θ_m and V_m values, which are : 7.44, 6.36, 5.7, 4.33, 3.56 V and 0.6, 0.4, 0.404, 0.33, 0.3 V for different temperatures 270, 300, 330, 360 and 390 K, respectively. The series resistance (Rs) is obtained from equation 15:

$$R_s = \frac{v_m}{I_m \theta_m^2} \tag{15}$$

We computed the values of barrier height (Φ_b), ideality factor (n) and series resistance (R_S) and reported them in Table 2. The obtained results (using I-V approach as example) between temperatures 270 K and 390 K, show an increase in barrier height

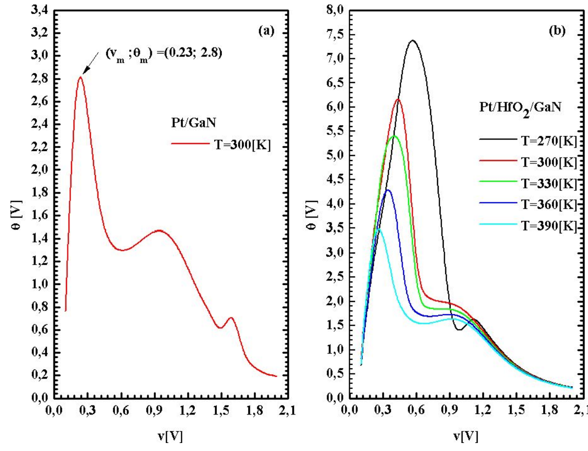

Fig. 5. Mikhelashvili's plots for (a) the Pt /GaN at T = 300 K and (b) the Pt /HfO_2/GaN for T= 270, 300, 330, 360 and 390 K.

(Φ_b) (from 0.74 to 0.87 eV), a decrease in ideality factor (n) (from 1.82 to 1.20) and a decrease in series resistance (R_S) (from 285 to 263 Ω). We observed that an increase in temperature is accompanied by a decrease in the ideality factor and increase in the barrier height for all methods. Statistical analysis results reveal that Pt/HfO_2/n-GaN structure has a higher rectification ratio with low reverse leakage current compared to Pt/n-GaN structure. The calculated barrier height of Pt/HfO_2/n-GaN structure (0.79 eV) is higher than Pt/n-GaN structure (0.56 eV) [22]. This relationship between temperature, barrier height and ideality factor is due to the inhomogeneity of barrier height resulting from Gaussian distribution of interfacial states at the M/SC interface [35]. The origin of this barrier height variation on Pt/HfO_2/n-GaN has been successfully explained on the basis of thermionic emission current (TE). This behavior is attributed to spatial variations of the barrier height [36]. We observed that the series resistance (Rs) value decreased with increasing temperature. This decrease can be due to the increasing of the free carrier concentration at high temperatures [37].

3.6. Inhomogeneous barrier analysis

The net current density j ($j = j_{sm} - j_{ms}$) through an inhomogeneous Schottky contact can be derived with the help of thermionic emission theory [37]. The density of the current (j_{sm}) flowing from the semiconductor into the metal across the band bending V, and the current (j_{ms}) from the metal to the semiconductor are written in the equation 16 [37]:

$$j_{sm} = A^*T^2 e^{-qV/kT} e^{-qV_d/kT} \tag{16}$$

and equation 17

$$j_{ms} = A^*T^2 e^{-q\varnothing_b/kT} \tag{17}$$

To have the percentages of potential distribution, we integrated j_{sm} over the potential V_d in equation 16. We get then the equation 18:

$$j_{sm} = A^*T^2 e^{-qv/kT} \int_{-\infty}^{\infty} e^{-qV_d/kT} P(V_d)\, dV_d \tag{18}$$

After integrating, equation 18 yields the effective band bending V_d^j for the current (j_{sm}) as written in equation 19:

$$V_d^j = \bar{v_d} - \frac{\sigma_s^2}{2kT/q} \tag{19}$$

Equation 18 can be rewritten as shown in equation 20:

$$j_{sm} = A^*T^2 e^{-qv/kT} e^{-qV_d^j/kT} \tag{20}$$

With similar integration of j_{sm} over the potential V_d of equation 17 we get equation 21:

$$\Phi_{ap} = \bar{\Phi}_{b0} - \frac{\sigma_s^2}{2kT} \tag{21}$$

where (σ_s) is the zero bias standard deviation of the BH distribution and it is a measure of the barrier homogeneity. The temperature dependence of (σ_s) is usually small and can be neglected. The voltage-independent ideality factor (n) requires a linear increase in $\Phi_b(V, T)$ with the bias.

This is only possible if the mean Schottky barrier height SBH (Φ_b), as well as the square of the standard deviation (σ_s), vary linearly with the bias [38, 39].

The observed variation of the ideality factor (n) with the temperature is given by equation 22 [38, 39]:

$$\frac{\partial \varnothing_{ap}}{\partial V} = \left(n_{ap}^{-1} - 1\right) = -\rho_2 + \frac{\rho_3 q}{2kT}, \tag{22}$$

where:

$$\Delta\Phi_b(v,T) = \Phi_b(v,T) - \Phi_b(0,T) \tag{23}$$

and

$$\Delta\sigma^2(v) = \sigma^2(v) - \sigma^2(0) = \rho_3 v \tag{24}$$

It is assumed that the mean SBH and the zero bias standard deviation are linearly bias dependent on Gaussian parameters such as $\bar{\Phi}_b = \rho_2 v + \Phi_{b0}$ and standard deviation $\sigma_s = \sigma_{s0} + \rho_3 v$ [38] where ρ_2 and ρ_3 are voltage coefficients which may be dependent on T. They quantify the voltage deformation of the barrier height distribution [40]. We calculated σ_{s0} – zero bias standard deviation, ρ_2 and ρ_3 voltage coefficients using I-V, Cheung, Chattopadhyay and Mikhelashvili schemes by fitting the nonlinear variation of Φ_b and $n^{-1} - 1$ versus $(2kT)^{-1}$ shown in Fig. 6. The results obey the variations presented in equations 25 and 26:

$$\begin{cases} \Phi_b^A = -0.009(2kT)^{-1} + 1.15 \\ \Phi_b^B = -0.013(2kT)^{-1} + 1.23 \\ \Phi_b^C = -0.006(2kT)^{-1} + 1.34 \\ \Phi_b^D = -0.0098(2kT)^{-1} + 1.07 \end{cases} \tag{25}$$

$$\begin{cases} (n^{-1} - 1)^A = -0.019(2kT)^{-1} + 0.45 \\ (n^{-1} - 1)^B = -0.019(2kT)^{-1} + 0.38 \\ (n^{-1} - 1)^C = -0.01(2kT)^{-1} + 0.10 \\ (n^{-1} - 1)^D = -0.014(2kT)^{-1} + 0.015 \end{cases} \tag{26}$$

where Φ_b^A is obtained by I-V method; Φ_b^B is obtained by Cheung method; Φ_b^C is obtained by Chattopadhyay method; Φ_b^D is obtained by Mikhelashvili method.

The obtained values of σ_s, ρ_2 and ρ_3 are presented in Table 3.

In this section, we calculated Richardson constant using two methods. The first - using conventional Richardson plot of the reverse saturation current [41] which can be written as shown in equation 27:

$$\ln\left(\frac{I_0}{T^2}\right) = \ln(AA^*) - \frac{q\varnothing_b}{kT} \tag{27}$$

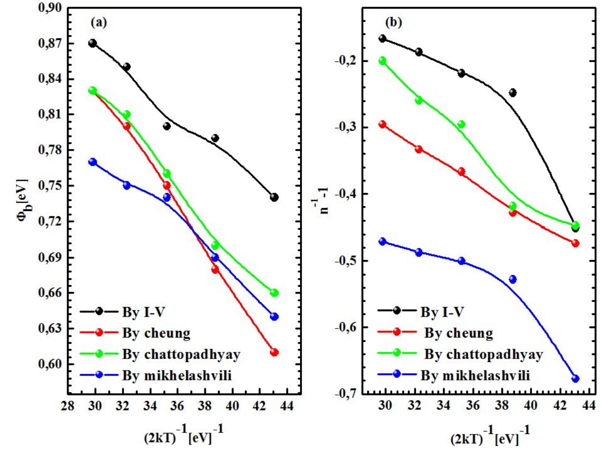

Fig. 6. (a) zero-bias apparent barrier height (Φ_b), (b) ideality factor ($n^{-1} - 1$) vs. 1/2kT plot for Pt/HfO_2/GaN

The plot of $\ln\left(\frac{I_0}{T^2}\right)$ vs. $\frac{1000}{T}$ is shown in Fig. 7a. We can get the value of Richardson constant (A^*) from the intercept of the straight portion of the curve (Fig. 7a) where we found the following value $0.51\ A \cdot cm^{-2}K^{-2}$.

The second method combines equation 2 and equation 21 to get equation 28:

$$\ln\left(\frac{I_0}{T^2}\right) - \left(\frac{q^2\sigma_s^2}{2kT^2}\right) = \ln(AA^*) - \frac{q\varnothing_b}{kT} \tag{28}$$

The modified Richardson plot $\ln\left(\frac{I_0}{T^2}\right) - \left(\frac{q^2\sigma_s^2}{2kT^2}\right) = \ln(AA^*) - \frac{q\varnothing_b}{kT}$ versus $\frac{1}{kT}$ shown in Fig. 7b, has quite a good linearity over the whole temperature range. The calculated Richardson constant (A^*) values using ((I-V), Cheung, Chattopadhyay and Mikhelashvili) methods are shown in Table 4.

4. Conclusions

Firstly, current-voltage characteristics of Pt/HfO_2/GaN have been simulated with the module ATLAS of SILVACO-TCAD in the temperature range 270 – 390 K by analyzing the parameters behavior with the temperature variation. We used different methods namely: conventional forward bias I-V, Cheung, Norde, Chattopadhyay, and Mikhelashvili to extract ideality factor (n), barrier

Table 3. Calculated values of standard deviation σ_s, ρ_2 and ρ_3 (voltage coefficients) in the temperature range of 270 K – 390 K.

Method	σ_s [eV]	ρ_2	ρ_3
I-V	0.097	-0.45	0.019
Cheung	0.114	-0.38	0.019
Chattopadhyay	0.078	-0.10	0.010
Mikhelashvili	0.088	0.015	0.014

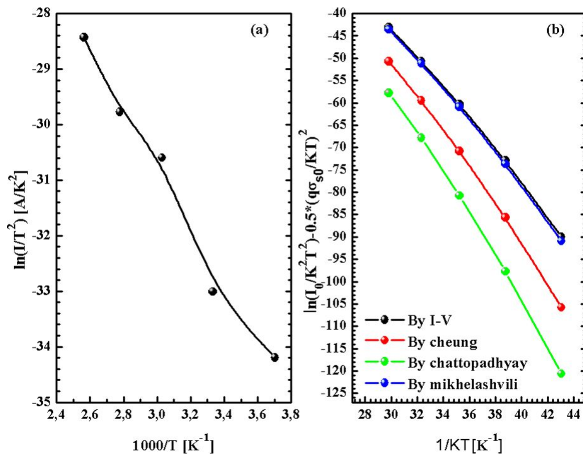

Fig. 7. (a) modified Richardson plots of $\ln\left(\frac{I_0}{T^2}\right)$ vs. (1000/T) and (b) $\ln\left(\frac{I_0}{T^2}\right) - \left(\frac{q^2\sigma_{s0}^2}{2kT^2}\right)$vs. (1/kT) for Pt/$HfO_2$/GaN in the temperature range 270 K – 390 K.

Table 4. The calculated values of the modified Richardson by the four methods

Methods	$A^*cm^{-2}K^{-2}$ Present work	Exp. [22]
I-V method	22.64	22.8
Cheung method	14.29	–
Chattopadhyay model	25.53	–
Mikhelashvili method	21.75	–

height (Φ_b) and series resistance (R_s). It was found that the ideality factor and series resistance of the diode decrease while the corresponding barrier height increases with increasing temperature. We observed that the insulator layer of HfO_2 caused an improvement in the performance of the diode by increasing the barrier height from 0.56 eV to 0.79 eV and decreasing the ideality factor from 2.01 to 1.33. In addition, the HfO_2 can be used as an interfacial layer to improve such parameters as rectification (BH) and ideality factor of a Pt/n-GaN. The obtained results have also shown that the linearity of Richardson plot ($\ln\left(\frac{I_0}{T^2}\right) - \left(\frac{q^2\sigma_s^2}{2kT^2}\right)$ versus $\frac{1}{kT}$) simulated by conventional forward bias I-V, Cheung, Chattopadhyay and Mikhelashvili methods is a consequence of the barrier inhomogeneity, which means that the inhomogeneity of the barrier does not affect the transport with temperature variation. Therefore, we obtained Richardson constant values in a close agreement with the known value of (26.4 $A\cdot cm^{-2}K^{-2}$ for n-type GaN) by Chattopadhyay method.

References

[1] ASUBAY S., GÜLLÜ Ö., TÜRÜT A., *Vacuum*, 83 (2009), 1470.

[2] ELHAJI A., EVANS-FREEMAN J. H., EL-NAHASS M.M., KAPPERS M. J., HUMPHRIES, *Mat. Sci. Semicon. Proc.*, 17(2014), 94.

[3] SCHLEEH J., ALESTIG G., HALONEN J., MALMROS A., NILSSON B., NILSSON P., STARSKI J.P., WADEFALK N., ZIRATH H., GRAHN J., *IEEE Electr. Device.*, 33 (2012), 664.

[4] KONCZYKOWSKA A., DUPUY J.-Y., JORGE F., RIET M., NODJIADJIM V., MARDOYAN H., *J. Lightwave Technol.*, 36 (2018), 401.

[5] PRASAD C V., REDDY M. S. P., REDDY V. R., PARK C., *Appl. Surf. Sci*, 427(2018), 670.

[6] ACAR F., BUYUKBAS-ULUSAN A., TATAROGLU A., *J. Mater. Sci., Mater. Electron.*,29 (2018),12553.

[7] ADACHI S., *Properties of semiconductor alloys, group-IV, III-V and II-VI semiconductors*, John Wiley & Sons, United Kingdom, 2009.

[8] HATTORI K. TORII Y., *Solid State Electron.*, 34 (1991), 527.

[9] SINGH A., REINHARDT K., ANDERSON W., *J. Appl. Phys.*, 68 (1990), 3475.

[10] ENOKI T., YOKOYAMA H., UMEDA Y., OTSUJI T., *Jpn. J. Appl. Phys.*, 37 (1998), 1359.

[11] PANDE K., *IEEE T. Electron. Dev.*, 27 (1980), 631.

[12] Zeghdar K., Dehimi L., Saadoune A., Sengouga N., *J. Semicond.*, 36 (2015), 124002.
[13] Balaram N., Reddy V. R., Reddy P. S., Janardhanam V., Choi C.-J., *Vacuum*, 152 (2018), 15.
[14] Houssa M., Pantisano L., Ragnarsson L. A., Degraeve R., Schram T., Pourtois G., de Gendt S., Groeseneken G., Heyns M. M., *Mater. Sci. Eng.*, 51 (2006), 37.
[15] Fadel M., Azim M. O. A., Omer O. A., Basily. R. R.,*Appl. Phys. A-Mater.*, 66 (1998), 335.
[16] Meng Z., Huang S., Liu Z., Zeng C., Bu Y., *Optoelectron. Lett.*, 8 (2012), 190.
[17] Reddy V. N., Padma R., Gunasekhar, *Appl. Phys. A-Mater.*, 124(2018), 79.
[18] Reddy V. R., Manjunath V., Janardhanam V., Kil Y. H., Choi C.-J., *Journal of Elec. Materi.*, 43(2014), 3499.
[19] Lakshmi B. P., Reddy V. R., Janardhanam V., Reddy M. S. P., Lee J. H., *Appl. Phys. A*, 113(2013), 713.
[20] Prasad C. V., Reddy V. R., Choi C.-J., *Appl. Phys. A*, (2017), 123.
[21] Reddy M.S.P., Puneetha P., Reddy V.R., Lee J.H., Jeong S.H., Park, *J. Electron. Mater.*, 45(2016), 5655.
[22] Shetty A., Roul B., Mukundan S., Mohan L., Chandan G., Vinoy K. J., Krupanidhi S. B., *AIP Adv.*, 5(2015), 097103.
[23] He G., Zhu L., Liu M., Fang Q., Zhang L., *Appl. Surf. Sci.*, 253 (2007), 3413.
[24] Mamor M., *J. Phys.-Condens. Mat.*, 21(2009), 335802.
[25] Monaghan S., Hurley P. K., Cherkaoui K., Negara M. A., Schenk A., *Solid State Electron.*, 53(2009), 438.
[26] Robertson J., *Eur. Phys. J. Appl. Phys.*, 28(2004), 265.
[27] Padma R., Lakshmi B. P., Reddy M. S. P., Reddy V. R., *Superlattice Microst.*, 56 (2013), 64.
[28] Reddy V. R., Manjunath V., Janardhanam V., Kil Y.-H., Choi C.-J., *J. Electron. Mater.*, 43 (2014), 3499.
[29] Gholami S., Khakbaz M., *International Scholarly and Scientific Research*, 5 (2011).
[30] Dogan H., Elagoz S., *Physica ELow Dimens. Syst. Nanostruct.*, 63(2014), 186.
[31] Fritah A., Saadoune A., Dehimi L., Abay B., *Philos. Mag.*, 96(2016), 2009.
[32] Cheung S., Cheung N., *Appl. Phys. Lett.*, 49 (1986), 85.
[33] Norde H., *J. Appl. Phys.*, 50 (1979), 5052.
[34] Chattopadhyay P., *Solid State Electron.*, 38 (1995), 739.
[35] Mikhelashvili V., Eisenstein G., Garber V., Fainleib S., Bahir G., Ritter D., Orenstein M., Peer A., *J. Appl. Phys.*, 85(1999), 6873.
[36] Huang W.-C., Lin T.-C., Horng C.-T., Li Y.-H., *Mat. Sci. Semicon. Proc.*, 16 (2013), 418.
[37] Janardhanam V., Kumar A. A., Reddy V. R., Reddy P. N., *J. Alloy. Compd.*, 485 (2009), 467.
[38] Dogan H., Elagoz S., *Physica E Low Dimens. Syst. Nanostruct.*, 63 (2014), 186.
[39] Werner J. H., Güttler H. H., *J. Appl. Phys.*, 69 (1991), 1522.
[40] Doğan H., Yildirim N., Orak İ., Elagöz S., Turut A., *Physica B Condens. Matter*, 457 (2015), 48.
[41] Zhu S., Detavernier C., Van Meirhaeghe R., Cardon F., Ru G.-P., Qu X.-P., Li B.-Z., *Solid State Electron.*, 44 (2000), 1807.

Received 2018-12-21
Accepted 2019-04-23